Chemistry & Biology
Article

Optimizing Glycosyltransferase Specificity via "Hot Spot" Saturation Mutagenesis Presents a Catalyst for Novobiocin Glycorandomization

Gavin J. Williams,[1] Randal D. Goff,[1] Changsheng Zhang,[1] and Jon S. Thorson[1,*]
[1]Laboratory for Biosynthetic Chemistry, Pharmaceutical Sciences Division, School of Pharmacy, National Cooperative Drug Discovery Program, University of Wisconsin-Madison, 777 Highland Avenue, Madison, WI 53705, USA
*Correspondence: jsthorson@pharmacy.wisc.edu
DOI 10.1016/j.chembiol.2008.02.017

SUMMARY

A comprehensive two-phase "hot spot" saturation mutagenesis strategy for the rapid evolution of glycosyltransferase (GT) specificity for nonnatural acceptors is described. Specifically, the application of a high-throughput screen (based on the fluorescent acceptor umbelliferone) was used to identify key amino acid hot spots that contribute to GT proficiency and/or promiscuity. Saturation mutagenesis of the corresponding hot spots facilitated the utilization of a lower-throughput screen to provide OleD prodigy capable of efficiently glycosylating the nonnatural acceptor novobiocic acid with an array of unique sugars. Incredibly, even in the absence of a high-throughput screen for novobiocic acid glycosylation, this approach rapidly led to improvements in the desired catalytic activity of several hundred-fold.

INTRODUCTION

Glycosylated secondary metabolites continue to serve as an important source for the discovery of new drugs. As a key element of these natural pharmacophores, the attached sugars are typically critical for biological activity, and subtle alterations in natural-product glycosylation can transform a natural agent's pharmacological properties, its molecular and cellular specificity, and even its mechanism of action (Ahmed et al., 2006; Thorson and Vogt, 2002; Weymouth-Wilson, 1997). "Glycorandomization" is an emerging method for natural-product glycodiversification that employs the inherent or engineered substrate promiscuity of anomeric kinases and nucleotidyltransferases for the in vitro synthesis of sugar nucleotide libraries. As the culminating step, this diverse range of sugar donors is processed by natural-product glycosyltransferases (GTs) to provide a library of variant natural-product glycosides (Griffith et al., 2005; Langenhan et al., 2005). The successful glycorandomization of glycopeptides (Fu et al., 2003), avermectins (Zhang et al., 2006a), and enediynes (Zhang et al., 2006b) highlights the notable promiscuity displayed by several natural-product GTs. Yet, attempts to utilize other natural-product GTs for glycorandomization have been severely restricted by the catalysts' stringent substrate specificity (Borisova et al., 2006; Yuan et al., 2005). For example, the noviosyltransferase NovM, which catalyzes the glycosylation of novobiocic acid (**1**) (Figure 1A) en route to novobiocin (**8**) (Figure 1D; Albermann et al., 2003; Freel Meyers et al., 2003), was found to accept only 4 of 54 alternative sugar nucleotides examined (Albermann et al., 2003; Freel Meyers et al., 2003). Thus, although permissive secondary metabolite GTs provide new opportunities for drug discovery, the stringent specificity of others limits enzymatic natural-product diversification and highlights a need for general GT engineering and/or evolution platforms.

Despite a wealth of GT structural and biochemical information, few successful applications of rational structure-based engineering to alter natural-product GT donor/acceptor specificities exist (Hancock et al., 2006; Williams and Thorson, 2008b). Among the most recent, a combination of sequence-guided and structure-guided mutagenesis allowed for the modulation of the *N*- versus *O*-glucosylation activities of xenobiotic GTs from *Arabidopsis thaliana* (Brazier-Hicks et al., 2007). Alternatively, the general lack of high-throughput GT screens/selections has also limited the directed evolution of GTs (Williams et al., 2007; Williams and Thorson, 2008a). As the first example in the context of natural products, the directed evolution of the oleandomycin GT (OleD) from *Streptomyces antibioticus* by using a simple fluorescence-based screen was recently described (Williams et al., 2007; Williams and Thorson, 2008a). Specifically, a small library of OleD variants, screened for the ability to glucosylate the fluorescent surrogate acceptor 4-methylumbelliferone (**4**), led to a number of variants with the improved ability to produce β-D-glucopyranoside (**6**) (Figure 1B). The functional amino mutations were subsequently recombined to afford a triple-mutant enzyme that displayed a marked improvement in both acceptor and donor promiscuity. Interestingly, this variant also displayed a modest (5-fold) improvement in glucosylation toward novobiocin aglycon (**1**) (Figure 1C)—a potential starting point for circumventing the stringency of the native noviosyltransferase NovM. Moreover, novobiocin presents an excellent model, as the aminocoumarins have long been known as potent bacterial type II DNA topoisomerase DNA gyrase inhibitors (Maxwell and Lawson, 2003) and can also augment the activity of various anticancer agents via their ability to inhibit Hsp90 (Marcu et al., 2000a, 2000b).

Unlike the umbelliferone **4**, novobiocic acid (**1**) is not fluorescent, which severely limits the throughput of any engineering strategy dependent upon **1** as substrate. We postulated that the amino acid positions identified (hot spots) as contributing to GT proficiency and/or promiscuity via the high-throughput fluorescence-based screen (using **4**) are also likely to contribute

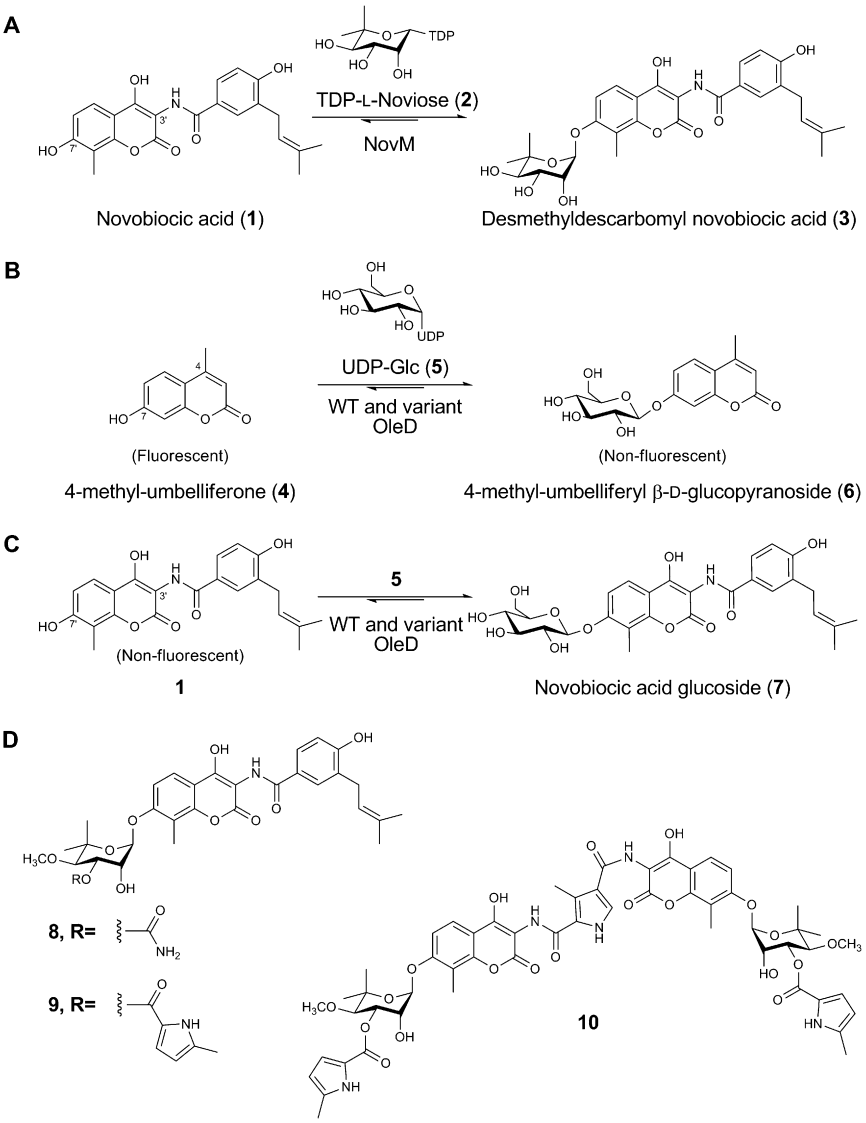

Figure 1. Relevant GT-Catalyzed Coumarin Glycosylation Reactions

(A) The reaction catalyzed by WT NovM.

(B) The reaction employed for the fluorescence-based screening assay used to evolve OleD.

(C) Representation of the novobiocic acid glucosylation reaction catalyzed by WT and variant OleD.

(D) The structures of the representative naturally occurring aminocoumarin antibiotics novobiocin (**8**), clorobiocin (**9**), and coumermycin A_1 (**10**).

to utilization of other variant substrates (e.g., **1**). To test this hypothesis, herein we describe the optimization of OleD toward the nonnatural acceptor **1** via a comprehensive program of hot spot saturation mutagenesis of functional positions previously identified via the high-throughput fluorescence-based screen. Incredibly, even in the absence of a high-throughput screen for glucosylation of **1**, this approach led to activity improvements toward **1** of several hundred-fold. In addition, this study reveals a correlation between catalyst proficiency and increased donor promiscuity in the context of **1**, ultimately affording a new, to our knowledge, catalyst for the glycorandomization of novobiocin.

RESULTS

Specificity of OleD Mutants toward Novobiocic Acid (1)

As previously described, the OleD triple mutant P67T/S132F/A242V displayed improvements in glucosylation activity with a panel of nonnatural acceptors, including novobiocic acid (**1**) (5-fold improved; Williams et al., 2007). This variant was constructed after the identification of three clones from a library of OleD mutants, which had improved activity toward umbelliferone **4**. One of these clones, 2C3, possessed a single amino acid mutation (A242V), whereas the other two, 8B3 and 7B9, possessed the mutations P67T/I112T and S132F/G340W, respectively. In order to identify functional mutations in 8B3 and 7B9, each single mutant was constructed by site-directed mutagenesis, and the specific activity of each purified enzyme toward **4** was determined (Williams et al., 2007). These results clearly demonstrated that P67T, S132F, and A242V were responsible for improved activity toward **4** (~7-, 2.6-, and 2.3-fold improved compared to wild-type [WT] OleD), whereas G340W and I112T appeared to be nonfunctional (~0.5-fold reduced activity, compared to WT OleD; Williams et al., 2007). To further evaluate the impact of these mutations on substrate specificity, the activity of each single mutant OleD was determined with the alternative acceptor, **1** (Figure 2A). These results revealed that P67T, S132F, and A242V increased production of the putative glucoside **7** 2- to 3-fold (Figure 2A), whereas G339W was nonbeneficial. Surprisingly, I112T displayed the largest improvement (7.4-fold) in glucosylation activity toward **1**. Thus, in the previously identified double mutant P67T/I112T (clone 8B3; Williams et al., 2007), both P67T and I112T influence **1** specificity, whereas only P67T appears to be functional with respect to **4**.

Given that I112T, P67T, S132F, and A242V individually improve activity toward **1**, combinations were next assessed for synergistic enhancements of the desired activity. For this secondary set of combinations, I112T was retained as an invariant substitution, given its significant impact on the activity of **1**. Thus, three double mutants were generated by combining P67T, S132F, and A242V with I112T, and each double mutant was overexpressed and purified, and the specific activity toward the substrate pair **1**/**5** was determined by reverse phase-high-performance liquid chromatography (RP-HPLC; Figure 2A). This analysis revealed that the activity of the I112T variant could

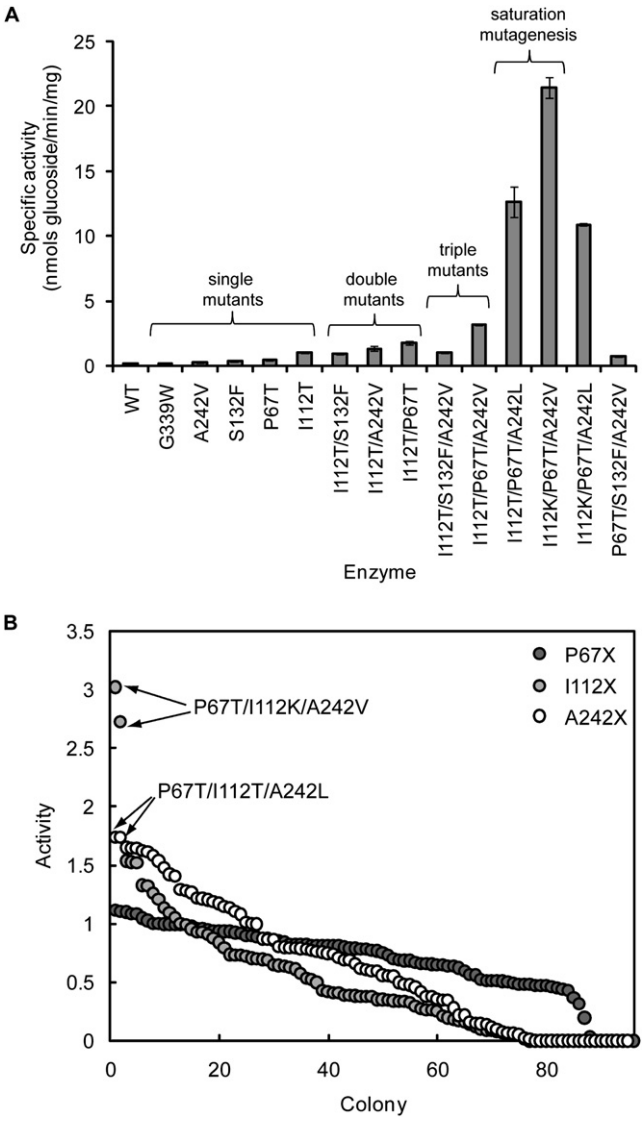

Figure 2. Creation of OleD Variants Improved toward Novobiocic Acid, 1

(A) Specific activities of WT and mutant OleDs with novobiocic acid (**1**) and UDP-Glc (**5**) as acceptor and donor, respectively. Error bars represent standard deviation from three independent measurements.

(B) The crude cell extract glucosylation activities of randomly selected colonies from saturation mutagenesis libraries P67X, I112X, and A242X, with **1** as the acceptor. Activities are illustrated in descending order, and arrows designate clones that were selected for in-depth characterization.

be further enhanced via the incorporation of either P67T or A242V (P67T/I112T and A242V/I112T, respectively), whereas the S132F/I112T variant was slightly less active than the I112T parent (Figure 2A). As predicted, further amalgamation of the three remaining mutations, to give the triple mutant P67T/I112T/A242V, provided a superior catalyst for **1** glucosylation. Among the two additional triple mutants possible, I112T/S132F/A242V was less active than P67T/I112T/A242V, consistent with the detrimental effect of the S132F mutation in combination with other functional substitutions. Therefore, the remaining triple mutant (P67T/I112T/S132F) was not pursued. For unknown reasons, the quadruple mutant P67T/I112T/S132F/A242V failed to express under several different conditions tested (data not shown).

Saturation Mutagenesis of Pro67, Ile112, and Ala242

To further optimize the selected lead catalyst, single-site saturation mutagenesis at Pro67, Ile112, and Ala242 in the scaffold P67T/I112T/A242V was performed, generating the libraries "P67X," "I112X," and "A242X," respectively. A key constraint of this approach is that, unlike the screening target in our original directed evolution program (**4**), the acceptor, **1**, is nonfluorescent. Accordingly, each library was screened for activity toward **1** via RP-HPLC, and, for convenience, we limited screening to ~100 colonies from each library, which represents ~95% coverage (Firth and Patrick, 2005). From this approach, library P67X failed to identify improved variants, whereas several colonies from the I112X and A242X libraries displayed 2- to 3-fold enhancements of **1** glucosylation (Figure 2B). DNA sequencing revealed that substitution of Ala242 with leucine was responsible for the hits identified from the A242X library, whereas two hits from the I112X library were found to possess the mutation I112K. Subsequent enzyme assay, with purified enzymes, confirmed that these clones were more active than the parent P67T/I112T/A242V. Specifically, P67T/I112K/A242V and P67T/I112T/A242L were ~7- and ~4-fold improved, respectively, over the parent P67T/I112T/A242V (Figure 2A). While a recombination of the three "best" mutations (P67T/I112K/A242L) leads to a slightly less active variant, it is notable that this approach rapidly identified a variant (P67T/I112K/A242V) that is 150-fold improved compared to WT OleD and 28-fold improved over the previously described P67T/S132F/A242V (Williams et al., 2007) in terms of specific activity with **1** and **5**.

Product Characterization

All OleDs described, including WT OleD, catalyzed the formation of a single, identical product based on RP-HPLC and liquid chromatography-mass spectrometry (LC-MS) (data not shown), consistent with the formation of a single monoglucoside with conserved regio- and stereochemistry. The architectural similarities between **1** and umbelliferone **4** implicate the **1** C7′-OH as the likely position for glucosylation, to provide **7** (Figure 1C). Scale-up of the P67T/I112K/A242L-catalyzed **1**-glucosylation reaction followed by structural elucidation confirmed glucoside **7** as the product (see Experimental Procedures and Figure S1, see the Supplemental Data available with this article online). Interestingly, LC-MS analysis of this large-scale reaction also revealed trace production of a putative diglucosyl-substituted product (data not shown).

Kinetic Characterization of WT and Mutant OleDs

The WT and the mutant OleD P67T/I112K/A242L were compared by determining steady-state kinetic parameters with **1** or **5** as variable substrates, as described in the Experimental Procedures. The WT enzyme displayed hyperbolic saturation with both **1** and **5** as variable substrates, providing a K_M for **1** and **5** of 2 and 2.81 mM, respectively (Figures 3A and 3B). The k_{cat}s determined with **1** and **5** (0.041 and 0.073 min^{-1}, respectively) were not in complete agreement, likely because at the concentration of **1** used (5 mM, the solubility limit), with **5** as variable substrate,

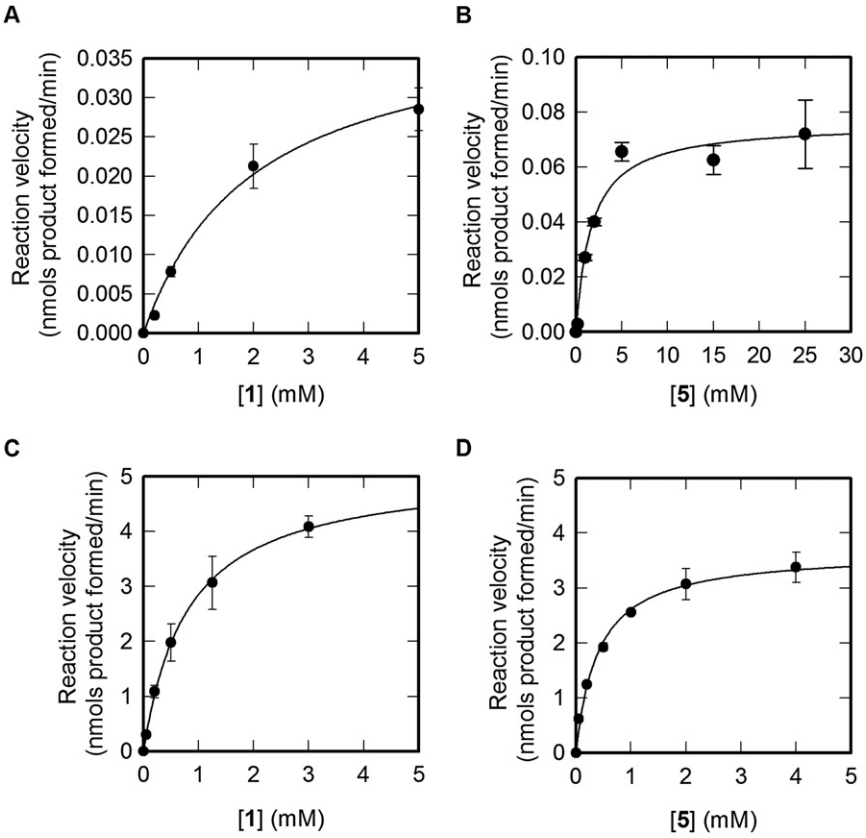

Figure 3. Steady-State Kinetic Analysis of WT and P67T/I112K/A242V OleD

(A) WT OleD with novobiocic acid (**1**) as variable substrate and the concentration of UDP-Glc (**5**) fixed at 5 mM.

(B) WT OleD with UDP-Glc (**5**) as variable substrate and the concentration of novobiocic acid (**1**) fixed at 5 mM.

(C) P67T/I112K/A242V OleD with novobiocic acid (**1**) as variable substrate and the concentration of UDP-Glc (**5**) fixed at 5 mM.

(D) P67T/I112K/A242V OleD with UDP-Glc (**5**) as variable substrate and the concentration of novobiocic acid (**1**) fixed at 5 mM.

Error bars represent standard deviation from three independent measurements.

WT OleD was not completely saturated with acceptor. Nevertheless, these results demonstrate that **1** is a poor substrate for WT OleD.

The steady-state kinetics of the triple mutant P67T/I112K/A242V were very different from that of the WT enzyme (Figures 3C and 3D). Saturation with both **1** and **5** was easily achieved, with apparent K_Ms of 0.8 mM and 0.41 mM, respectively, which are 2.5-fold and 6.9-fold improved over WT OleD. Moreover, the k_{cat}s determined with either acceptor **1** or donor **5** as the variable substrate (5.13 and 3.67 min^{-1}) were in closer agreement, reflecting the improved K_M for the acceptor. Thus, in terms of catalytic efficiency (k_{cat}/K_M) with **1** as acceptor, the triple mutant P67T/I112K/A242V is ~300-fold improved compared to WT OleD.

Donor Specificity of P67T/I112K/A242V

The sugar nucleotide donor promiscuity of WT and mutant P67T/I112K/A242V OleD was probed by using RP-HPLC analysis with a set of 20 potential "unnatural" UDP donors as surrogates for UDP-Glc (**5**) in the presence of **1** as acceptor (Figure 4A). This set was comprised of unnatural sugar nucleotides generated via chemoenzymatic synthesis, representing alterations of the sugar at C1″, C2″, C3″, C4″, or C6″ (Barton et al., 2002; Fu et al., 2003; Jiang et al., 2003). Putative product identities were confirmed by LC-MS (Figure S2; Table S1). Of the 21 sugar nucleotides tested, only UDP-Glc (**5**), UDP-xylose (**11**), UDP-6-deoxy-glucose (**12**), and UDP-4,6-dideoxy-glucose (**18**) led to detectable product with WT OleD, ranging from ~0.1%–3% conversion in 3 hr (Figure 4B). In contrast, the optimized mutant P67T/I112K/A242V accepted 10 of 21 sugar nucleotide donors examined, 6 of which were not detectable substrates of WT OleD, with improvements in conversion ranging from 10- to 375-fold (Figure 4B; Table S1).

Proficiency and Promiscuity

A subset of donors (**5**, **11**, **15**, **21**, and **22**), representing diverse sugar modifications, was employed to further probe the donor promiscuity of several OleD variants by using **1** as the acceptor. The variants selected included WT, the optimal triple mutant P67T/I112K/A242V (Figure 4B), the previously described P67T/S132F/A242V (Williams et al., 2007), and the scaffold for saturation mutagenesis (P67T/I112T/A242V) to represent a "family" of mutant OleDs with gradual improvements in proficiency toward the substrate pair **1**/**5**. This analysis revealed that WT OleD accepts only two members of the donor subset (**2** and **11**, Figures 4A–4C), whereas the mutant P67T/S132F/A242V was ~5-fold improved toward donor **5**, slightly enhanced with **11**, and also accepted **15** (albeit poorly; Figure 4C). Replacing S132F with I112T in this triple mutant, P67T/S132F/A242V, further improved activity toward **5**, **11**, and **15** (Figure 4C). The final optimal mutant (P67T/I112K/A242V) afforded by saturation mutagenesis displayed further improvements toward **5**, **11**, **15** and detectable turnover with **22** (Figures 4A–4C). None of the mutants displayed any detectable activity toward **21**.

DISCUSSION

Directed evolution has proven to be an effective tool for altering the specificity of enzymes and presents a possible solution for overcoming the strict specificity of certain GTs such as NovM (Rubin-Pitel and Zhao, 2006). However, the success of directed evolution is distinctly dependent on the availability of a suitable high-throughput screen or selection for the desired activity. This is especially problematic in the context of GTs, given the huge variety of glycosyl donors and acceptors utilized by this large family of enzymes (Hu and Walker, 2002; Williams and Thorson, 2008b). For example, in the case of novobiocin, the aglycon **1** and any corresponding glycoside (e.g., **7**) are indistinguishable

spectrophotometrically. Interestingly, the recently successful directed evolution of the macrolide GT OleD, based on a simple fluorescent acceptor surrogate (**4**), led to the discovery of an OleD variant that displayed a modest (5-fold) improvement in **1** glucosylation (Williams et al., 2007). This pioneering study served not only as a potential starting point for circumventing the stringency of the native noviosyltransferase NovM, but it also suggested that the amino acid positions identified (hot spots) as contributing to GT proficiency and/or promiscuity via the high-throughput fluorescence-based screen (using **4**) may also contribute to utilization of other variant substrates (e.g., **1**). Notably, whereas positions identified by random mutagenesis and screening/selection for a desired activity have often been further optimized by saturation mutagenesis/recombination (Chica et al., 2005), the application of the secondary saturation mutagenesis/recombination to optimize a completely distinct activity (e.g., utilization of a very different nonnatural substrate) has not been reported.

Of the mutations identified in the initial directed evolution study with fluorescent surrogate **4** (P67T, I112T, S132F, A242V, G340W; Williams et al., 2007), the first four individually contributed to improved glycosylation of **1**, with I112T as the most active single mutant. It should be mentioned that, given the low mutation rates and limited library sizes typically employed in directed evolution strategies, it is uncommon to find multiple functional mutations in the same clone. Yet, both P67T and I112T, originally discovered as a combination in the single clone 8B3, improved activity with **1**. Subsequent combinations of P67T, S132F, and A242V, on an invariant I112T background, led to catalyst P67T/I112T/A242V, which displayed a 22-fold improvement in specific activity toward **1** compared to WT OleD. Saturation mutagenesis at Pro67, Ile112, and Ala242 on the same background revealed additional gains via incorporation of polar/charged amino acids at position 112 (I112T or I112K) and increasing hydrophobic steric bulk at residue 242 (A242L). In contrast, variation of Pro67 failed to improve the desired activity under the conditions employed. Although this preliminary analysis is consistent with P67T as the optimal substitution, it is also possible that other mutations at Pro67 simply did not improve the rate of glucosylation at the concentration of acceptor/donor used (i.e., mutations could improve K_M, but not k_{cat}). Interestingly, a final combination of the optimized mutations (I112K and A242L) was slightly detrimental to activity under the assay conditions used, as P67T/I112K/A242L was less active than both P67T/I112K/A242V and P67T/I112T/A242L. Yet, the final optimized variant (P67T/I112K/A242V) displayed a 150-fold improved specific activity toward **1** compared to WT OleD. Steady-state kinetic analysis illustrated that P67T/I112K/A242V is 200- or 300-fold more efficient (in terms of k_{cat}/K_M) with UDP-Glc (**5**) or acceptor **1**, respectively, compared to WT OleD, and this change reflected improvements in both k_{cat} and K_M for donor and acceptor.

Using the high-throughput fluorescence-based "surrogate" screen to first identify functional hot spots notably limited the low-throughput catalyst optimization to screening only ~300 colonies via HPLC. As a comparison, analysis of the OleD-macrolide complex structure implicates at least 32 residues (including the acceptor binding pocket and "loop N3") as being key to forming the static acceptor binding site (Figure 5) in an "open" conformation (Bolam et al., 2007). Thus, to simply assess the single best amino acid at each of the 32 structure-designated positions via saturation mutagenesis would require screening >3000 colonies (32 × 100 for ~95% coverage) by HPLC. Among the hot spots identified via the fluorescence-based screen, the OleD structure reveals Ile112 to be intimately associated with acceptor binding (Figure 5), and the previous mutation of an equivalent residue (Ile117) in oleandomycin GT OleI (45% identity with OleD) reduced k_{cat}/K_M by ~100-fold (Bolam et al., 2007). Pro67 is part of the substrate-binding "loop N3" (amino acids 60–76) following β sheet 3 in the N-terminal domain (Figure 5), and a similarly located proline has been implicated in controlling the substrate specificity of urdamycin GTs (Hoffmeister et al., 2002). Structural analysis does not predict the synergistic/antagonistic influences of S132 and/or the A242 optimal substitutions for activity toward **1**/**5** and may also exclude certain dynamic elements/residues critical for catalysis. Thus, although both structure-guided and directed-evolution approaches may ultimately arrive at many of the same mutations, the hot spot-focused strategy described herein may present a more streamlined approach for catalyst optimization.

It has been previously suggested that naturally occurring GTs with high turnover numbers will be more promiscuous (Oberthür et al., 2005). The availability of a unique family of OleD variants displaying a gradient of catalytic efficiencies from this study allowed for a more direct test of this hypothesis. As illustrated in Figure 4C, enhancements in NDP-sugar donor promiscuity indeed paralleled the improvements in catalyst proficiency, culminating in a catalyst capable of accepting 11 of 21 UDP donors tested (compared to only trace conversion of 4 UDP donors by WT OleD). Although this study is consistent with the notion that more proficient GTs are generally promiscuous, it is also important to note that several naturally occurring GTs display very high efficiency yet remain exquisitely selective. For example, WT NovM with its natural substrates TDP-L-noviose (**2**) and **1** is ~3 orders of magnitude more proficient than the triple mutant P67T/I112K/A242V with **1** and **5**, based on k_{cat}/K_M, but displays a remarkably narrow substrate specificity range (Freel Meyers et al., 2003). On the other hand, P67T/I112K/A242V is ~1 order of magnitude more efficient (in terms of k_{cat}/K_M toward **1** and **5**) than WT NovM toward an alternative donor, TDP-6-deoxy-glucose (Albermann et al., 2003), and approaches the catalytic efficiency of other natural-product GTs, such as the relatively promiscuous teicoplanin GT tGtfb (Howard-Jones et al., 2007).

With respect to the importance of aminocoumarin glycosylation, the 2″-, 3″-, and 4″-noviose moieties are critical for maintaining the antibacterial activity of **8** (Freitag et al., 2004; Galm et al., 2004a; Xu et al., 2004), whereas removal of **8**, 3-carbamoyl moiety of noviose, increases Hsp90 inhibition ≥ 70-fold (Burlison et al., 2006; Yu et al., 2005). Glycosyl-modified **8** analogs also provide potent neuroprotective activities (Ansar et al., 2007). Yet, although the potential value of varying aminocoumarin glycosylation clearly exists, pathway engineering and semisynthetic efforts to date have led to fairly conservative glycosyl modifications (Galm et al., 2004b). The present study sets the stage to greatly expand upon the availability of differentially glycosylated aminocoumarins. For example, glucoside **7** and the glycosides derived from donors **15**, **18**, **19**, **22**, **23**, **24**, and **28** from this proof of concept study have not been previously described. Access to these compounds may further the therapeutic development of aminocoumarins and could also be used to interrogate the

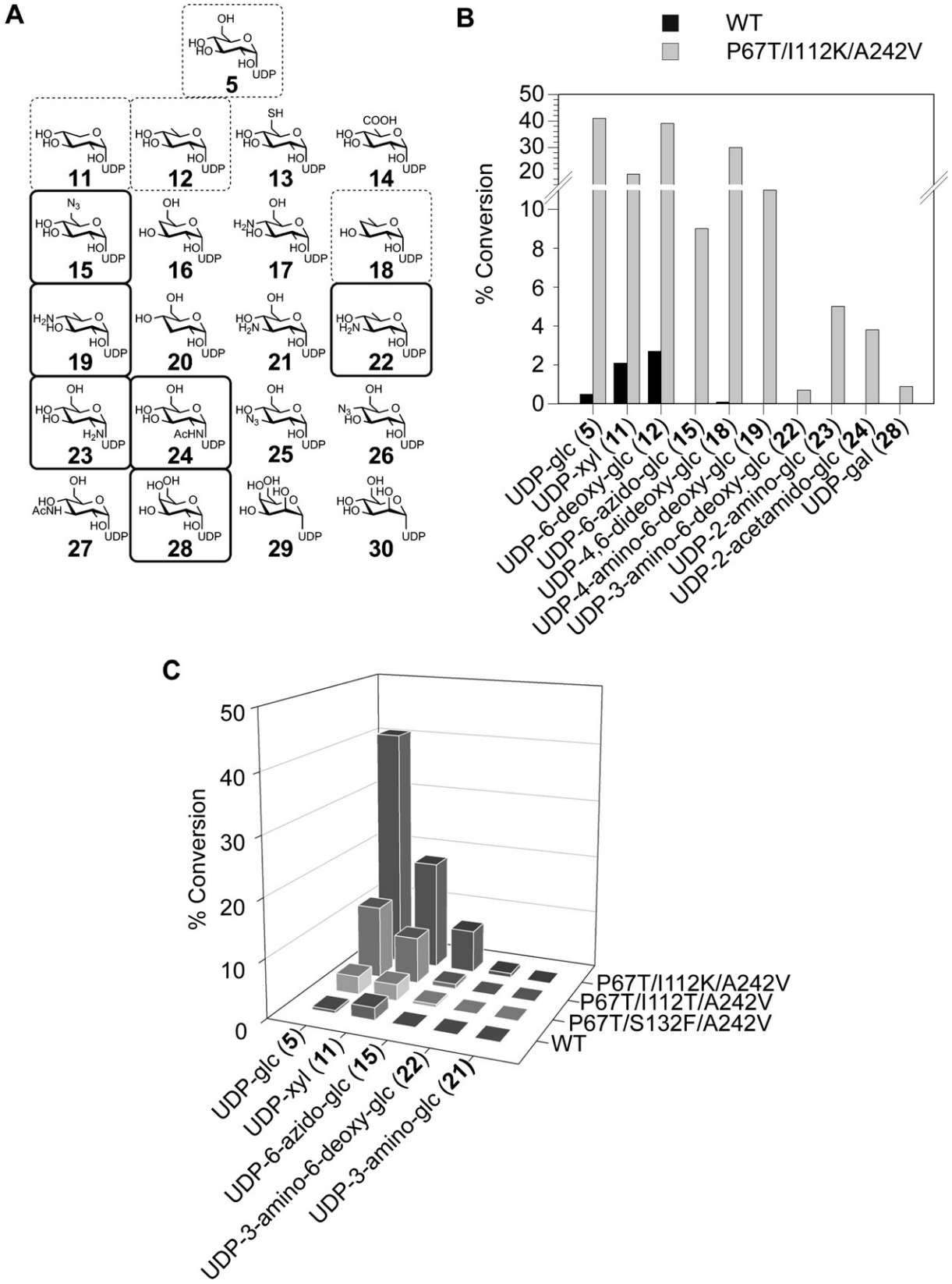

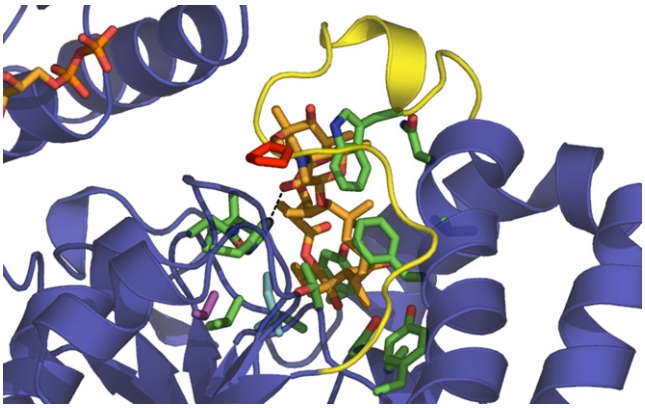

Figure 5. OleD Active Site Structure
The key residues delineated in this study are highlighted within the previously reported active site structure of OleD bound to oleandomycin and NDP (PDB code: 21YF). Color designations—substrates, orange; Pro-67, red; Ile-112, cyan; Ser-132, magenta; loop N3, yellow; dashed line, H-bond between the catalytic His-25 and acceptor sugar-OH. Residues in green are those that form the acceptor binding pocket, which is largely hydrophobic.

specificity of late-stage aminocoumarin biosynthetic-modifying enzymes, such as the acyltransferase CouN7 (Balibar et al., 2007; Fridman et al., 2007), toward further diversification. Utilization of UDP-6-azido-glucose (**15**) as a new substrate also presents the potential for further downstream chemoselective diversification (Fu et al., 2003).

SIGNIFICANCE

Using the macrolide GT OleD as a model, this study unveils a general enzyme optimization strategy (hot spot saturation mutagenesis) applicable to reactions limited by amenable high-throughput screens. Specifically, the application of a high-throughput screen (based on the fluorescent acceptor umbelliferone) was used to identify key amino acid hot spots that contribute to GT proficiency and/or promiscuity. Saturation mutagenesis of the corresponding hot spots facilitated the utilization of a lower-throughput screen (based on the acceptor novobiocic acid) to provide OleD prodigy capable of efficiently catalyzing the production of a novel set of differentially glycosylated aminocoumarins—an important class of natural products with known antibiotic, anticancer, and antineurodegenerative activities. A systematic comparison of OleD variants from this study also revealed the first, to our knowledge, direct correlation between catalyst proficiency and increased donor promiscuity. As this work demonstrates a platform for the rapid generation of new glycosylation catalysts, the concept of hot spot saturation mutagenesis as applied herein should be broadly applicable in the context of new catalyst development.

EXPERIMENTAL PROCEDURES

General

Bacterial strain *E. coli* BL21(DE3)pLysS was purchased from Stratagene. NovaBlue was purchased from Novagen. Plasmid pET28/OleD was a generous gift from Professor Hung-Wen Liu (University of Texas-Austin, Austin, USA), and pET28a was purchased from Novagen. All other chemicals were reagent grade and were purchased from Fluka, New England Biolabs, or Sigma unless otherwise stated. Primers were ordered from Integrated DNA Technologies (Coralville, IA). Novobiocic acid (**1**) was prepared as previously described from novobiocin (Albermann et al., 2003). Product standard 4-methyl-umbelliferyl-7-*O*-β-D-glucoside (**6**) and UDP-Glc (**5**) were purchased from Sigma. Analytical HPLC was performed on a Rainin Dynamax SD-2/410 system connected to a Rainin Dynamax UV-DII absorbance detector. Mass spectra were obtained by using electrospray ionization on an Agilent 1100 HPLC-MSD SL quadrupole mass spectrometer connected to a UV/Vis diode array detector. For LC-MS analysis, quenched reaction mixtures were analyzed by analytical RP-HPLC with a 250 mm × 4.6 mm Gemini 5μ C18 column (Phenomenex, Torrance, CA) by using a gradient of 10%–90% CH_3CN in 0.1% formic acid/H_2O for 20 min at 1 ml/min, with detection at 254 nm. Structural characterization was performed by NMR spectroscopy using a Varian ^{UNITY}*INOVA* 500 MHz instrument (Palo Alto, CA) in conjunction with a Protasis/MRM CapNMR capillary probe (Savoy, IL). The spectrum was referenced to DMSO-d_6 at 2.50 ppm.

Site-Directed Mutagenesis

Site-specific OleD variants were constructed by using the Stratagene QuikChange II Site-Directed Mutagenesis Kit, as described by the manufacturer. Constructs were confirmed to carry the correct mutation(s) via DNA sequencing.

Saturation Library Preparation

The saturation mutagenesis libraries "P67X," "I112X," and "A242X" were constructed by using the Stratagene QuikChange II Site-Directed Mutagenesis Kit, as described by the manufacturer, with the mutant P67T/I112T/A242V as template. For each library, plasmid DNA (digested with DpnI) was transformed into Novablue chemical competent cells, and the transformants were grown overnight at 37°C on LB agar supplemented with 50 μg/ml kanamycin. Colonies from each library were subsequently pooled and used to inoculate 5 ml LB medium supplemented with 50 μg/ml kanamycin for overnight growth at 37°C with shaking (350 rpm). Using standard mini-prep purification, the mixed-population plasmid prep was prepared from each 5 ml culture and transformed into *E. coli* BL21(DE3)pLysS, and the transformants were grown overnight at 37°C on LB agar supplemented with 50 μg/ml kanamycin.

For protein expression, individual colonies from plates containing BL21(DE3)pLysS transformants were subsequently used to inoculate wells of a 96-deep well microtiter plate, wherein each well contained 1 ml LB medium supplemented with 50 μg/ml kanamycin. Culture plates were tightly sealed with AeraSeal breathable film (Research Products International Corp.). After cell growth at 37°C for 18 hr with shaking at 350 rpm, 100 μl of each culture was transferred to a fresh deep-well plate containing 1 ml LB medium supplemented with 50 μg/ml kanamycin. The original plate was sealed and stored at 4°C, or a glycerol copy was made by mixing 100 μl of each culture with 100 μl 50% (v/v) glycerol and was stored at −80°C. The freshly inoculated plate was incubated at 37°C for 2–3 hr with shaking at 350 rpm. Protein expression was induced at an OD_{600} of ~0.7, isopropyl β-D-thiogalactoside (IPTG) was added to a final concentration of 0.4 mM, and the plate was incubated for 18 hr at 18°C. Cells were harvested by centrifugation at 3000 × g for 10 min at 4°C, the cell pellets were thoroughly resuspended in chilled 50 mM Tris-HCl (pH 8.0) containing 10 mg/ml lysozyme (Sigma), and the plates were

Figure 4. Probing the Donor Specificity of WT OleD and Mutant Prodigy
(A) The set of UDP-sugar donors used to probe specificity. Dashed-boxed donors were detectable substrates for both WT and mutant P67T/I112T/A242V OleD, whereas solid-boxed donors were substrates only for P67T/I112T/A242V.
(B) Successful conversion rates (%) after 3 hr with WT or P67T/I112T/A242V OleD by using 50 μM acceptor **1** and 250 μM UDP-sugar donors (the reactions containing **28** were incubated for 18 hr).
(C) Improvement of donor promiscuity with increasing proficiency of OleD variants.

subjected to a single freeze/thaw cycle to lyse the cells. After thawing, cell debris was collected by centrifugation at 3000 × g for 20 min at 4°C, and 50 μl of the cleared supernatant was used for the enzyme assay.

For crude extract assays, cleared supernatant was mixed with an equal volume (50 μl) of 50 mM Tris-HCl (pH 8.0) containing 10 mM $MgCl_2$, 200 μM **1**, and 1.0 mM **5** by using a Biomek FX Liquid Handling Workstation (Beckman Coulter, Fullerton, CA). Upon mixing, the reactions were incubated for 3 hr at 30°C, at which point the crude reaction mixture was mixed with an equal volume of MeOH and centrifuged at 3000 × g for 20 min at 4°C. Aliquots of each product mixture (40 μl) were analyzed by RP-HPLC as described below for determination of specific activity.

Protein Expression and Purification

For the characterization of specific OleD variants, single colonies were used to inoculate 3 ml LB medium supplemented with 50 μg/ml kanamycin and were cultured overnight at 37°C. The entire starter culture was then transferred to 1 l LB medium supplemented with 50 μg/ml kanamycin and were grown at 37°C until the OD_{600} was ~0.7, IPTG to a final concentration of 0.4 mM was added, and the flask was incubated for 18 hr at 18°C. Cell pellets were collected by centrifugation at 10,000 × g and 4°C for 20 min; resuspended in 10 ml 20 mM phosphate buffer (pH 7.4), containing 0.5 M NaCl and 10 mM imidazole; and were lysed by sonication. Cell debris was removed by centrifugation at 10,000 × g at 4°C for 30 min, and the cleared supernatant was immediately applied to 2 ml nickel-nitrilotriacetic acid (Ni-NTA) resin (QIAgen Valencia, CA), pre-equilibrated with lysis buffer. Protein was allowed to bind for 30 min at 4°C with gentle agitation, and the resin was washed four times with 50 ml lysis buffer. Finally, the enzyme was eluted by incubation of the resin with 2 ml lysis buffer containing 100 mM imidazole for 10 min at 4°C with gentle agitation. The purified enzyme was applied to a PD-10 desalting column (Amersham Biosciences AB) equilibrated with 50 mM Tris-HCl (pH 8.0) and eluted as described by the manufacturer. Protein aliquots were immediately flash frozen in liquid nitrogen and stored at −80°C. Protein purity was verified by SDS-PAGE. Protein quantification was carried out by using the Bradford Protein Assay (Bio-Rad, Hercules, CA).

Determination of Specific Activity with 1 or 4 as Acceptor

Enzyme reactions were carried out in a total volume of 100 μl 50 mM Tris-HCl (pH8.0) containing 5 mM $MgCl_2$, 200 μM **1** or **4**, 5 mM **5**, and, typically, 10–50 μg pure enzyme. At a suitable time interval during which the rate of product formation was linear with time (typically 2–20 min), reactions were quenched with 100 μl MeOH, and the samples were centrifuged at 10,000 × g for 10 min. Supernatants were analyzed by analytical RP-HPLC with a Gemini 5μ C18 column (Phenomenex) by using a gradient of 10%–90% CH_3CN in 0.1% trifluoroacetic acid (TFA)/H_2O for 20 min, with detection at 254 nm. Under these conditions, substrates **1** (t_R = 25.5 min) or **4** (t_R = 14.5 min) and the glucoside products **7** (t_R = 18.8 min) or **6** (t_R = 9.95 min) were readily resolved. The identity of **7** was confirmed by LC-MS and NMR, whereas the density of glucoside **6** was confirmed by coelution with a commercial standard and LC-MS analysis. HPLC peak areas were integrated, and the product concentrations were calculated as a percentage of the total peak area. Specific activity was expressed as nanomoles product formed/min/mg protein.

Scale-Up and Characterization of Glucoside 7

The preparative reaction to synthesize the novobiocyl glucoside (**7**) was accomplished at room temperature in a total volume of 10 ml in 50 mM Tris-HCl (pH 8.0) containing 5 mM $MgCl_2$, 10 mg novobiocic acid (**1**), 60 mg UDP-Glc (**5**), and 5 mg purified OleD mutant P67T/I112T/A242V. The reaction was incubated for 48 hr, after which protein was removed by adding 30 ml cold MeOH and by centrifugation at 10,000 × g and 4°C for 30 min. The supernatant was concentrated, lyophilized, and resuspended in 1 ml DMSO, and the sample was purified by HPLC by using a Gemini 5μ C18 column (Phenomenex) with a gradient of 10%–90% CH_3CN in 0.1% trifluoroacetic acid (TFA)/H_2O for 20 min, with detection at 254 nm. The product fractions were pooled and lyophilized. ^{1}H NMR (1:2 DMSO-d_6:CD_3OD) δ7.69 (br s, 1 H, H_5''), 7.66 (br s, 1 H, H_2), 7.50 (m, 1 H, H_6), 7.09 (br d, J = 7.1 Hz, 1 H, H_6'), 6.69 (m, 1 H, H_5), 5.24 (br s, 1 H, H_8), 4.90 (d, J = 6.9 Hz, 1 H, H_1''), 3.75 (d, J = 11.5 Hz, 1 H, H_{6a}''), 3.56 (m, 1 H, H_{6b}''), 3.36 (m, 4 H, $H_{2''-5''}$), 3.27 (m, 2 H, H_7), 2.09 (s, 3 H, H_{11}'), 1.62 (s, 6 H, $H_{10,11}$). The anomeric coupling constant and NOESY are consistent with the C7-β-glucoside (**7**) (see Figure S1).

Determination of Kinetic Parameters

Enzyme assays were carried out in a total volume of 100 μl 50 mM Tris-HCl (pH 8.0) containing 5 mM $MgCl_2$ and, typically, 10–50 μg pure enzyme. Kinetic parameters k_{cat} and K_M were determined with both **1** and **5** as variable substrates. For the determination of K_M for **1**, **5** was constant at 5 mM and **1** varied between 0.025 and 5 mM. For the determination of K_M for **5**, **1** was constant at 5 mM and **5** varied between 0.05 and 25 mM. Each experiment was performed in triplicate. Aliquots (100 μl) were removed between 0 and 30 min, at which time product formation was still linear with respect to time; quenched with 100 μl ice-cold MeOH, and centrifuged at 10,000 × g for 10 min. Supernatants were analyzed by analytical RP-HPLC as described above. The substrate **1** and the glucoside product **7** HPLC peak areas were integrated, and the product concentration was calculated as a percent of the total peak area. Initial velocities were fitted to the Michaelis-Menten equation by using Sigma Plot.

Donor Specificity

To assess donor specificity, assays contained 50 μM acceptor **1** and ~500 μM putative NDP-sugar donor in a total assay volume of 50 μl. For this study, the NDP sugars were used directly from RmlA-catalyzed reactions (Barton et al., 2002; Fu et al., 2003; Jiang et al., 2003). Although **11**, **14**, and **24** were also commercially available, low levels of contamination with UDP-Glc in the commercial reagents complicated product analysis by LC-MS (data not shown), and, therefore, the RmlA-derived **11**, **14**, and **24** were utilized. Reactions were incubated at 25°C for 3 hr. Aliquots (25 μl) were quenched with 25 μl ice-cold MeOH and were centrifuged at 10,000 × g for 10 min. Supernatants were analyzed by analytical RP-HPLC as described above. HPLC peak areas were integrated, and the product concentration was calculated as a percent of the total peak area. All products were characterized by LC-MS.

SUPPLEMENTAL DATA

Supplemental Data include NOESY of novobiocic acid glucoside **7** and RP-HPLC/LC-MS analysis of WT and mutant OleD donor specificity and are available at http://www.chembiol.com/cgi/content/full/15/4/393/DC1/.

ACKNOWLEDGMENTS

We are grateful to the School of Pharmacy Analytical Instrumentation Center for analytical support. This work was supported in part by National Institutes of Health grants AI52218 and U19 CA113297. J.S.T is a University of Wisconsin H.I. Romnes Fellow. The authors report competing interests. J.S.T. is a cofounder of Centrose (Madison, WI).

Received: January 9, 2008
Accepted: February 22, 2008
Published: April 18, 2008

REFERENCES

Ahmed, A., Peters, N.R., Fitzgerald, M.K., Watson, J.A., Jr., Hoffmann, F.M., and Thorson, J.S. (2006). Colchicine glycorandomization influences cytotoxicity and mechanism of action. J. Am. Chem. Soc. *128*, 14224–14225.

Albermann, C., Soriano, A., Jiang, J., Vollmer, H., Biggins, J.B., Barton, W.A., Lesniak, J., Nikolov, D.B., and Thorson, J.S. (2003). Substrate specificity of NovM: implications for novobiocin biosynthesis and glycorandomization. Org. Lett. *5*, 933–936.

Ansar, S., Burlison, J.A., Hadden, M.K., Yu, X.M., Desino, K.E., Bean, J., Neckers, L., Audus, K.L., Michaelis, M.L., and Blagg, B.S.J. (2007). A non-toxic Hsp90 inhibitor protects neurons from Aβ-induced toxicity. Bioorg. Med. Chem. Lett. *17*, 1984–1990.

Balibar, C.J., Garneau-Tsodikova, S., and Walsh, C.T. (2007). Covalent CouN7 enzyme intermediate for acyl group shuttling in aminocoumarin biosynthesis. Chem. Biol. *14*, 679–690.

Barton, W.A., Biggins, J.B., Jiang, J., Thorson, J.S., and Nikolov, D.B. (2002). Expanding pyrimidine diphosphosugar libraries via structure-based nucleotidylyltransferase engineering. Proc. Natl. Acad. Sci. USA *99*, 13397–13402.

Bolam, D.N., Roberts, S., Proctor, M.R., Turkenburg, J.P., Dodson, E.J., Martinez-Fleites, C., Yang, M., Davis, B.G., Davies, G.J., and Gilbert, H.J. (2007). The crystal structure of two macrolide glycosyltransferases provides a blueprint for host cell antibiotic immunity. Proc. Natl. Acad. Sci. USA *104*, 5336–5341.

Borisova, S.A., Zhang, C., Takahashi, H., Zhang, H., Wong, A.W., Thorson, J.S., and Liu, H.W. (2006). Substrate specificity of the macrolide-glycosylating enzyme pair DesVII/DesVIII: opportunities, limitations, and mechanistic hypotheses. Angew. Chem. Int. Ed. Engl. *45*, 2748–2753.

Brazier-Hicks, M., Offen, W.A., Gershater, M.C., Revett, T.J., Lim, E.K., Bowles, D.J., Davies, G.J., and Edwards, R. (2007). Characterization and engineering of the bifunctional *N*- and *O*-glucosyltransferase involved in xenobiotic metabolism in plants. Proc. Natl. Acad. Sci. USA *104*, 20238–20243.

Burlison, J.A., Neckers, L., Smith, A.B., Maxwell, A., and Blagg, B.S. (2006). Novobiocin: redesigning a DNA gyrase inhibitor for selective inhibition of Hsp90. J. Am. Chem. Soc. *128*, 15529–15536.

Chica, R.A., Doucet, N., and Pelletier, J.N. (2005). Semi-rational approaches to engineering enzyme activity: combining the benefits of directed evolution and rational design. Curr. Opin. Biotechnol. *16*, 378–384.

Firth, A.E., and Patrick, W.M. (2005). Statistics of protein library construction. Bioinformatics *21*, 3314–3315.

Freel Meyers, C.L., Oberthur, M., Anderson, J.W., Kahne, D., and Walsh, C.T. (2003). Initial characterization of novobiocic acid noviosyl transferase activity of NovM in biosynthesis of the antibiotic novobiocin. Biochemistry *42*, 4179–4189.

Freitag, A., Galm, U., Li, S.M., and Heide, L. (2004). New aminocoumarin antibiotics from a cloQ-defective mutant of the clorobiocin producer *Streptomyces roseochromogenes* DS12.976. J. Antibiot. (Tokyo) *57*, 205–209.

Fridman, M., Balibar, C.J., Lupoli, T., Kahne, D., Walsh, C.T., and Garneau-Tsodikova, S. (2007). Chemoenzymatic formation of novel aminocoumarin antibiotics by the enzymes CouN1 and CouN7. Biochemistry *46*, 8462–8471.

Fu, X., Albermann, C., Jiang, J., Liao, J., Zhang, C., and Thorson, J.S. (2003). Antibiotic optimization via in vitro glycorandomization. Nat. Biotechnol. *21*, 1467–1469.

Galm, U., Dessoy, M.A., Schmidt, J., Wessjohann, L.A., and Heide, L. (2004a). In vitro and in vivo production of new aminocoumarins by a combined biochemical, genetic, and synthetic approach. Chem. Biol. *11*, 173–183.

Galm, U., Heller, S., Shapiro, S., Page, M., Li, S.M., and Heide, L. (2004b). Antimicrobial and DNA gyrase-inhibitory activities of novel clorobiocin derivatives produced by mutasynthesis. Antimicrob. Agents Chemother. *48*, 1307–1312.

Griffith, B.R., Langenhan, J.M., and Thorson, J.S. (2005). 'Sweetening' natural products via glycorandomization. Curr. Opin. Biotechnol. *16*, 622–630.

Hancock, S.M., Vaughan, M.D., and Withers, S.G. (2006). Engineering of glycosidases and glycosyltransferases. Curr. Opin. Chem. Biol. *10*, 509–519.

Hoffmeister, D., Wilkinson, B., Foster, G., Sidebottom, P.J., Ichinose, K., and Bechthold, A. (2002). Engineered urdamycin glycosyltransferases are broadened and altered in substrate specificity. Chem. Biol. *9*, 287–295.

Howard-Jones, A.R., Kruger, R.G., Lu, W., Tao, J., Leimkuhler, C., Kahne, D., and Walsh, C.T. (2007). Kinetic analysis of teicoplanin glycosyltransferases and acyltransferase reveal ordered tailoring of aglycone scaffold to reconstitute mature teicoplanin. J. Am. Chem. Soc. *129*, 10082–10083. Published online July 28, 2007. 10.1021/ja0735857.

Hu, Y., and Walker, S. (2002). Remarkable structural similarities between diverse glycosyltransferases. Chem. Biol. *9*, 1287–1296.

Jiang, J., Albermann, C., and Thorson, J.S. (2003). Application of the nucleotidylyltransferase Ep toward the chemoenzymatic synthesis of dTDP-desosamine analogues. ChemBioChem *4*, 443–446.

Langenhan, J.M., Griffith, B.R., and Thorson, J.S. (2005). Neoglycorandomization and chemoenzymatic glycorandomization: two complementary tools for natural product diversification. J. Nat. Prod. *68*, 1696–1711.

Marcu, M.G., Chadli, A., Bouhouche, I., Catelli, M., and Neckers, L.M. (2000a). The heat shock protein 90 antagonist novobiocin interacts with a previously unrecognized ATP-binding domain in the carboxyl terminus of the chaperone. J. Biol. Chem. *275*, 37181–37186.

Marcu, M.G., Schulte, T.W., and Neckers, L. (2000b). Novobiocin and related coumarins and depletion of heat shock protein 90-dependent signaling proteins. J. Natl. Cancer Inst. *92*, 242–248.

Maxwell, A., and Lawson, D.M. (2003). The ATP-binding site of type II topoisomerases as a target for antibacterial drugs. Curr. Top. Med. Chem. *3*, 283–303.

Oberthür, M., Leimkuhler, C., Kruger, R.G., Lu, W., Walsh, C.T., and Kahne, D. (2005). A systematic investigation of the synthetic utility of glycopeptide glycosyltransferases. J. Am. Chem. Soc. *127*, 10747–10752.

Rubin-Pitel, S.B., and Zhao, H. (2006). Recent advances in biocatalysis by directed enzyme evolution. Comb. Chem. High Throughput Screen. *9*, 247–257.

Thorson, J.S., and Vogt, T. (2002). Glycosylated natural products. In Carbohydrate-Based Drug Discovery, C.-H. Wong, ed. (Weinheim: Wiley-VCH), pp. 685–712.

Weymouth-Wilson, A.C. (1997). The role of carbohydrates in biologically active natural products. Nat. Prod. Rep. *14*, 99–110.

Williams, G.J., Zhang, C., and Thorson, J.S. (2007). Directed evolution of a natural product glycosyltransferase. Nat. Chem. Biol. *3*, 657–662.

Williams, G.J., and Thorson, J.S. (2008a). A high-throughput fluorescence-based glycosyltransferase screen and its application in glycosyltransferase directed-evolution. Nat. Protocols *3*, 357–362.

Williams, G.J., and Thorson, J.S. (2008b). Natural product glycosyltransferases: properties and applications. Adv. Enzymol. Relat. Areas Mol. Biol. *76*, in press.

Xu, H., Heide, L., and Li, S.M. (2004). New aminocournarin antibiotics formed by a combined mutational and chemoenzymatic approach utilizing the carbamoyltransferase novN. Chem. Biol. *11*, 655–662.

Yu, X.M., Shen, G., Neckers, L., Blake, H., Holzbeierlein, J., Cronk, B., and Blagg, B.S. (2005). Hsp90 inhibitors identified from a library of novobiocin analogues. J. Am. Chem. Soc. *127*, 12778–12779.

Yuan, Y., Chung, H.S., Leimkuhler, C., Walsh, C.T., Kahne, D., and Walker, S. (2005). In vitro reconstitution of EryCIII activity for the preparation of unnatural macrolides. J. Am. Chem. Soc. *127*, 14128–14129.

Zhang, C., Albermann, C., Fu, X., and Thorson, J.S. (2006a). The in vitro characterization of the iterative avermectin glycosyltransferase AveBI reveals reaction reversibility and sugar nucleotide flexibility. J. Am. Chem. Soc. *128*, 16420–16421.

Zhang, C., Griffith, B.R., Fu, Q., Albermann, C., Fu, X., Lee, I.K., Li, L., and Thorson, J.S. (2006b). Exploiting the reversibility of natural product glycosyltransferase-catalyzed reactions. Science *313*, 1291–1294.